Optical trapping and manipulation of atoms near surfaces

Cornelussen, R.A.

Publication date
2004

5 Power-efficient frequency switching of a locked laser

This chapter has been published as:

R.A. Cornelussen, T.N. Huussen, R.J.C. Spreeuw,
and H.B. van Linden van den Heuvell,
Appl. Phys. B **78**, 19 (2004).

We demonstrate a new and efficient laser-locking technique that enables making large frequency jumps while keeping the laser in lock. A diode laser is locked at a variable offset from a Doppler-free spectral feature of rubidium vapor. This is done by frequency shifting the laser before sending the light to a spectroscopy cell with an acousto-optic modulator (AOM). The frequency of the locked laser is switched quasi-instantaneously over much more than the width of the spectral features, i.e. the usual locking range. This is done by simultaneously switching the AOM frequency and applying feedforward to the laser current. The advantage of our technique is that power loss and beam walk caused by the AOM do not affect the main output beam, but only the small fraction of light used for the spectroscopy. The transient excursions of the laser frequency are only a few MHz and last approximately 0.2 ms, limited by the bandwidth of our locking electronics. We present equations that describe the transient behavior of the error signal and the laser frequency quantitatively. They are in good agreement with the measurements. The technique should be applicable to other types of lasers.*

5.1 Introduction

For the purpose of nowadays ubiquitous laser-cooling experiments [1, 3, 4] lasers are routinely locked to a Doppler-free absorption feature of an atomic transition. In a typical experimental time sequence one would first accumulate atoms into a magneto-optical trap (MOT) followed by a phase of e.g. polarization-gradient cooling. Both phases require different detunings of the laser light. The required switching of the frequency has been solved in several ways. However the existing solutions have some disadvantages, especially in terms of efficiency of laser power.

An existing and straightforward method is to lock the laser to a fixed detuning away from resonance and shift the laser frequency towards resonance by a variable amount, using an acousto-optic modulator (AOM). Usually the AOM is used in double-pass configuration to cancel beam walk associated with frequency shifting, resulting in a limited efficiency, typically lower than 65%. Moreover the beam walk compensation is imperfect.

Both the loss of laser power and the residual beam walk can be a problem when the light is used directly in an experiment, or when high-power multi-mode amplifier lasers are used, such as a broad-area laser (BAL) [101, 102] or a semiconductor tapered-amplifier laser (TA) [103]. With more seeding power such amplifiers perform better in terms of spectral purity and output power. Moreover they impose strict requirements on the beam pointing stability of the injection beam. The latter problem could be solved by first amplifying the light before frequency shifting it, providing the amplifier with sufficient power and a stably aligned injection beam. However power loss and beam walk now occur in the amplified beam.

Another solution is to injection lock [104, 105, 106] a second single-mode diode laser with the frequency shifted light, since this puts less stringent requirements on injection power and beam pointing stability. This injection-locked diode laser can subsequently be used to seed a BAL or TA laser [102]. A drawback is that this solution requires a significant amount of extra equipment. Furthermore, it is not possible to implement this solution in commercial BAL or TA systems without making major adjustments to the system, because the master laser is integrated in the system.

In this paper we demonstrate our method which is both efficient in its use of laser power and rigorously eliminates the beam walk due to the AOM frequency switching. We lock our laser using Doppler-free saturation spectroscopy in a vapor cell of rubidium. The laser is frequency shifted by an AOM before sending it through the spectroscopy cell. Thus, instead of shifting a fixed-frequency laser by a variable amount, we lock the laser at a variable frequency. This is only possible if the laser can follow the change in lock point associated with a change in the AOM frequency. This is a problem if the frequency jump is larger than the locking range set by the width of the Doppler-free features in the spectrum. We solved this by providing the laser with a feedforward signal, causing the laser to jump to within the locking range of the shifted lock point. We analyze the transient behavior of the laser frequency when making these jumps.

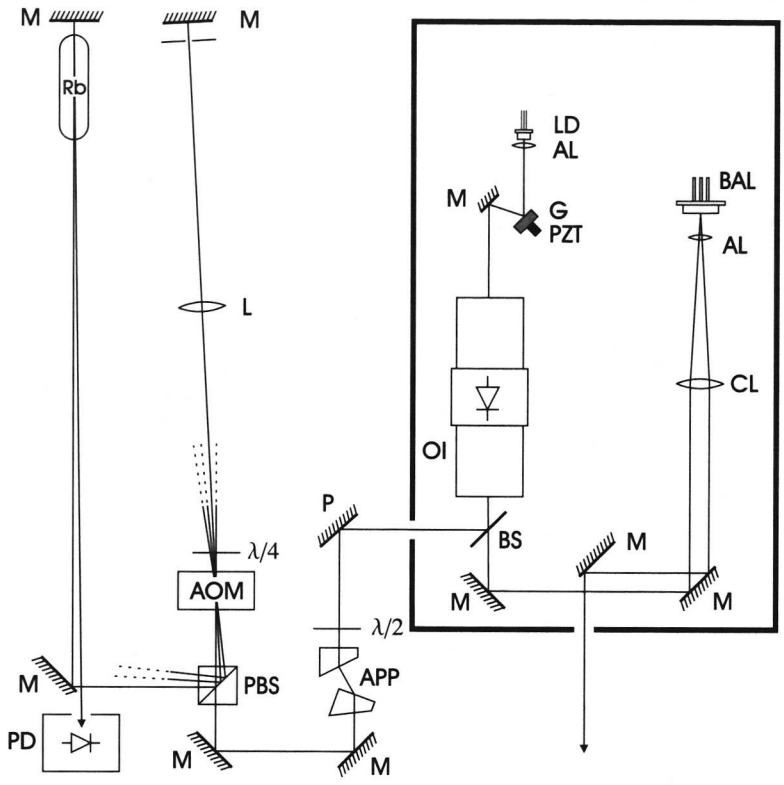

Figure 5.1: Schematic representation of the spectroscopy setup. The spectroscopy beam is sent through a double pass AOM setup to a saturated absorption section. This allows locking of the laser to an arbitrary frequency in the vicinity of an atomic transition. AL: aspheric lens, AOM: acousto-optic modulator, APP: anamorphic prism pair, BAL: broad area laser, BS: beam splitter, CL: cylinder lens, G: grating, L: lens, LD: laserdiode, M: mirror, OI: optical isolator, P: periscope, PBS: polarizing beam splitter, PD: photodiode, PZT: piezo transducer, Rb: cell with rubidium vapor.

5.2 Experimental implementation

In our experiment we work with ^{87}Rb which has a natural linewidth of $\Gamma/2\pi = 6$ MHz on the $5S_{1/2} \rightarrow 5P_{3/2}$ resonance line (D_2, 780 nm). The laser detunings needed for the MOT and the molasses phase are -1.5Γ and -10Γ with respect to the $F = 2 \rightarrow F' = 3$ component of the D_2 line. In view of the frequency range of our AOM we lock the spectroscopy beam to the $F = 2 \rightarrow F' = (1, 3)$ cross-over. The detunings with respect to this transition are 203 MHz and 152 MHz, respectively. The desired frequency jump of ~ 50 MHz is thus much larger than the locking range of about $\Gamma/2\pi$.

We use a commercial laser system (*Toptica*, PDL100) consisting of an extended cavity diode laser [91, 92] in Littrow configuration [93], which injection locks a BAL.

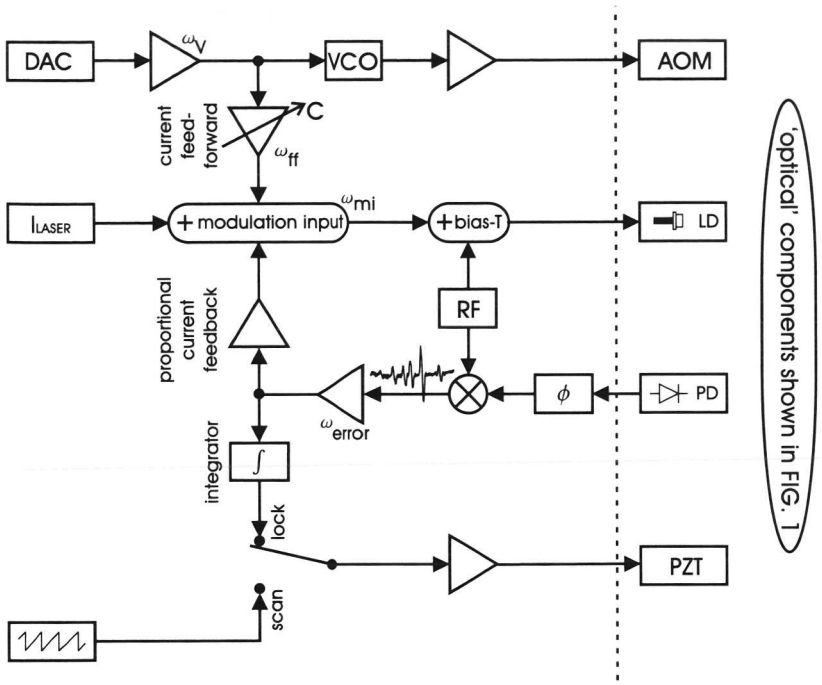

Figure 5.2: Schematic representation of the locking electronics. We employ FM spectroscopy to obtain a dispersive signal. This signal is used for integrational feedback to the PZT, and for proportional feedback to the laser current. The AOM frequency is generated by a VCO. The voltage driving the VCO is amplified and used as feedforward to the laser current in order to compensate the spectroscopy frequency for the frequency change of the AOM. On the left side of the dashed line the locking electronics is shown, on the right side the 'optical' components that can also be found in Fig. 5.1 are visible.

The grating of the extended cavity is mounted on a piezo stack (PZT) in order to scan the frequency. The setup is shown in Fig. 5.1. Behind the 60 dB optical isolator, 35 mW of power is left. The beam splitter reflects 10% to the spectroscopy setup. The spectroscopy beam first passes an anamorphic prism pair to circularize the elliptic beam shape. It then goes to a double pass AOM setup and finally to a Doppler-free spectroscopy section.

Fig. 5.2 shows a schematic representation of the electronics to lock the laser frequency. We employ FM spectroscopy [94, 95] to lock the laser. A small modulation with a radio frequency (RF) of 33 MHz is added to the laser current by means of a bias-T. The photodiode signal of the Doppler-free spectroscopy is phase shifted and mixed with the RF frequency resulting in a dispersive error signal, which is amplified with a measured bandwidth $\omega_{\text{error}}/2\pi \approx 20$ kHz. This signal is integrated and sent to the PZT in order to lock the laser to a spectral feature. Proportional current feedback is also applied to suppress fast fluctuations of the laser frequency. The AOM frequency is generated by a voltage controlled oscillator (VCO). The voltage

driving the VCO is generated by a 12 bit digital to analog convertor (DAC), which is subsequently converted to the correct voltage range. This last step has a measured bandwidth $\omega_V/2\pi = 2.6$ kHz.

Fig. 5.3(a) shows FM spectra measured by scanning the PZT for two AOM detunings δ_{AOM}, which are close to the frequencies used in a typical lasercooling experiment: $\delta_0/2\pi = -186.2$ MHz and $(\delta_0 + \delta_1)/2\pi = -137.4$ MHz. The jump in frequency is clearly larger than the half-width of the dispersive features, so that the locking electronics will not be able to keep the laser locked to the same line when this frequency jump is made. When this shift is compensated by applying a feedforward jump to the laser current the spectroscopy beam will not change frequency and the laser will stay locked. Experimentally this is done by attenuating the voltage driving the VCO (measured bandwidth of the attenuator $\omega_{ff}/2\pi = 125$ kHz) and feeding this as feedforward to the modulation input of the current controller, which has a specified bandwidth $\omega_{mi}/2\pi = 100$ kHz. Ideally the frequency change due to feedforward δ_{ff} and the AOM detuning δ_{AOM} should cancel. In reality the two frequencies are only approximately equal:

$$\delta_{ff} = -C\delta_{AOM}, \tag{5.1}$$

with $C \approx 1$. The parameter C is coarsely adjusted to 1 by optimizing the overlap of the two spectra. The accuracy is limited by the noise on the curves. Spectra with C adjusted to 1 by this method are shown in Fig. 5.3(b). When using the feedforward on the laser current, we observe that the laser remains locked while jumping. In the next section the transient behavior of the error signal will be discussed. A more accurate method to optimize C will be demonstrated in section 5.4.

5.3 Analysis of transient behavior

In this section an equation will be derived describing the transient behavior of the error signal. When the laser is locked to a dispersive spectral feature and the frequency excursions are small with respect to the width of this feature, the error signal $e(t)$ can be approximated by

$$e(t) = A(\omega_S(t) - \omega_R), \tag{5.2}$$

with A the slope of the dispersive signal of the reference feature at frequency ω_R, which is equal to the $F = 2 \rightarrow F' = (1, 3)$ cross-over frequency in our experiment. The frequency $\omega_S(t)$ of the light in the spectroscopy section is given by

$$\omega_S(t) = \omega_L(t) + \delta_{AOM}(t), \tag{5.3}$$

where $\omega_L(t)$ is the laser frequency and $\delta_{AOM}(t)$ is the shift in the double-pass AOM section. In our experiment this is a step function

$$\delta_{AOM}(t) = \delta_0 + \delta_1 u(t). \tag{5.4}$$

with $\delta_0/2\pi = -186.2$ MHz, $\delta_1/2\pi = 48.8$ MHz and $u(t)$ the unit step function, so that the laser changes frequency at $t = 0$. Including all feedback and feedforward terms the laser frequency $\omega_L(t)$ is given by

$$\omega_L(t) = \omega_0 + \varphi e(t) + \alpha \int_{-\infty}^{t} e(\tau)\mathrm{d}\tau + \delta_{ff}(t). \tag{5.5}$$

Here ω_0 is the frequency of the laser when it is not locked or any other electronic feedback is applied, the second term represents proportional current feedback. The third term is the integrational feedback to the PZT controlled grating. The last term is the feedforward to the laser current, which should instantaneously compensate the detuning jump by the AOM, as defined in Eq. (5.1).

When the laser is locked at $t = 0$, before the frequency jump, several terms cancel:

$$\omega_L(0_-) = \omega_0 + \varphi e(0_-) + \alpha \int_{-\infty}^{0} e(\tau)\mathrm{d}\tau - C\delta_0 = \omega_R - \delta_0. \tag{5.6}$$

Combining Eqs. (5.1)-(5.6) yields:

$$e(t) = A\left(\varphi e(t) + \alpha \int_{0}^{t} e(\tau)\mathrm{d}\tau + (1-C)\delta_1 u(t)\right) \tag{5.7}$$

from which the error function $e(t)$ after the frequency jump can be solved. As discussed in the previous section, several of the components have a limited bandwidth, which can be easily incorporated in the Laplace transform of Eq. (5.7), yielding

$$E(s) = \tau_{error}(s)A \times \left[\left(\tau_{mi}(s)\varphi + \frac{\alpha}{s}\right)E(s) + \tau_V(s)\left(1 - \tau_{mi}(s)\tau_{ff}(s)C\right)\frac{\delta_1}{s}\right], \tag{5.8}$$

with $E(s)$ the Laplace transform of $e(t)$ and $\tau_x(s) = 1/(1 + s/\omega_x)$ for $x \in \{error, V, ff, mi\}$ a (dimensionless) transfer function that describes the bandwidth of various components of the setup as shown in Fig. 5.2. Only the most limiting bandwidths are taken into account. The closed loop transfer function can be derived by solving $E(s)$ from Eq. (5.8). Subsequently the error function $e(t)$ can be derived from $E(s)$ by an inverse Laplace transformation. Although the solution $e(t)$ is analytical, it is not printed here, because it is too lengthy.

The frequency of the laser $\omega_L(t)$ can be derived from the error function by combining the Laplace transforms of Eqs. (5.2), (5.3) and (5.4) and incorporating the bandwidth transfer functions $\tau_x(s)$ as discussed previously. This yields for the laser frequency

$$\omega_L(t) = \mathcal{L}^{-1}\left(\frac{E(s)}{\tau_{error}(s)A} - \tau_V(s)\frac{\delta_1}{s}\right) + \omega_R - \delta_0, \tag{5.9}$$

where $\mathcal{L}^{-1}(\cdot)$ denotes an inverse Laplace transformation and the solution of Eq. (5.8) for $E(s)$ should be used for $E(s)$. Also Eq. (5.9) yields an analytical but lengthy solution, and is therefore not printed here. In the next section we will compare the calculated transients with the measured ones.

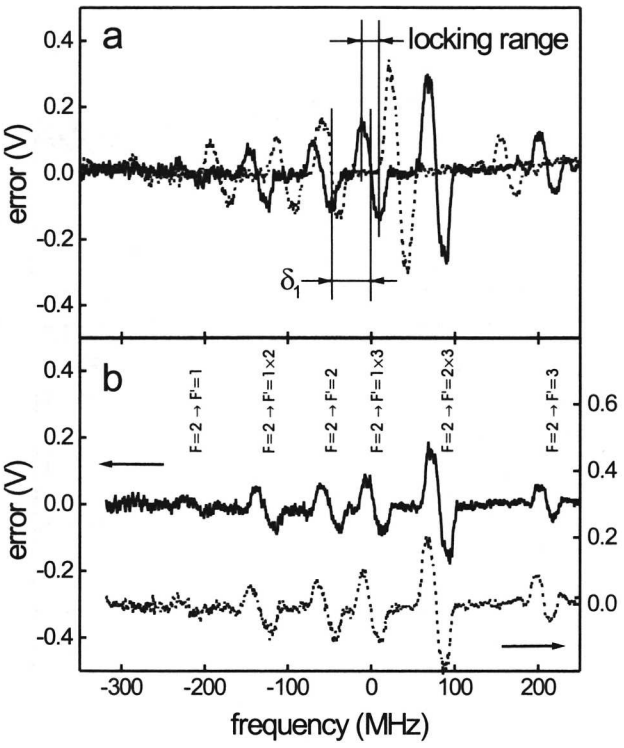

Figure 5.3: FM spectra, measured by scanning the PZT, for two different AOM detunings (a) without and (b) with current feedforward. It is clear that the frequency jump δ_1 is larger than the locking range, the width of the dispersive features. The laser will thus not stay locked to the $F = 2 \rightarrow F' = (1, 3)$ cross-over when the AOM frequency is changed without current feedforward. Note that the curves in (b) have been displaced vertically relative to each other.

5.4 Comparison with experimental data

To lock the laser while the AOM frequency is switching, first the parameter C is coarsely adjusted by overlapping the spectra as described in section 5.2 (see also Fig. 5.3(b). We then lock the laser to the desired zero crossing of the error signal by closing the feedback loop. While the laser is locked, the current feedback parameter φ is increased in order to decrease excursions of the error signal. The optimal value of φ is just below the value where the error signal starts to oscillate, in order to be as close as possible to critical damping. The top curve in Fig. 5.4(a) shows an error signal when the laser has been locked by this procedure and the frequency of the laser is changed from MOT to molasses frequency at $t = 0$. The error

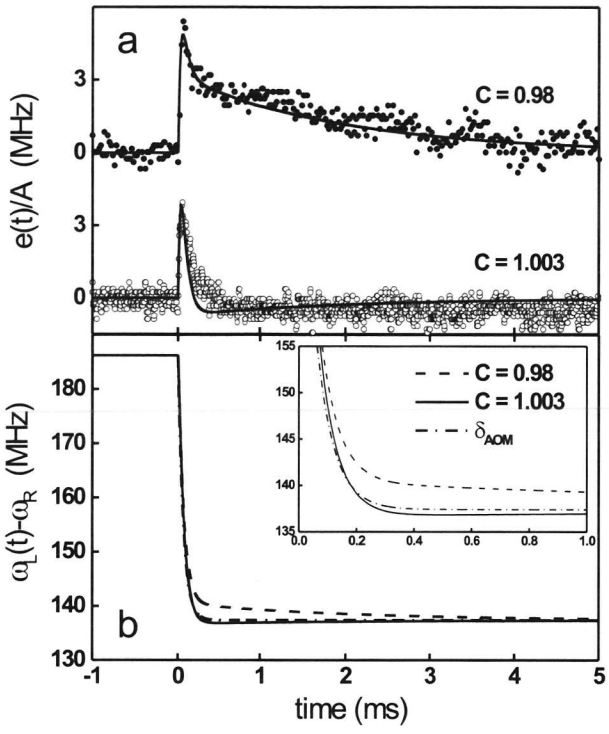

Figure 5.4: (a) Error signals versus time. At $t = 0$ the AOM and diode laser are switched from MOT detuning to molasses detuning. The top curve shows the error signal and a fit when the feedforward compensates 98% of the applied AOM shift, the bottom curve when the feedforward is 100.3% of the applied AOM shift. The solid line is the prediction of Eq. (5.8). (b) Laser frequency versus time for the above mentioned cases of current feedforward (solid and dashed), calculated using Eq. (5.9), and the frequency shift of the AOM (dash-dot), which is limited by the bandwidth of the step function ω_V. The inset shows the development of the laser frequency during the first millisecond in more detail.

signal is converted to a frequency by dividing it by the slope A of the dispersive signal. From this graph it is clear that in steady state the excursions of the laser frequency are approximately 1 MHz. One recognizes a fast increase of detuning due to the frequency shift of the AOM, followed by a decrease of frequency shift, because the current feedforward starts to compensate the AOM frequency shift. The current feedforward is slower than the AOM shift due to the bandwidths ω_{ff} and ω_{mi}. Finally a long tail due to the slow integrational feedback that removes the last amounts of the error signal is visible. It is clear that the current feedforward does not completely cancel the AOM detuning, resulting in a finite error signal that is

cancelled by the slow integrational feedback. By minimizing the amplitude of the error signal while the laser is locked and the AOM detuning is jumping, C can be optimized to a few permille. A curve with C optimized by using this method is shown in the bottom graph of Fig. 5.4(a). In order to determine values for C for both curves, fits to the data using the error signal $e(t)$ derived from Eq. (5.8) were performed. The results are shown as solid lines in Fig. 5.4(a). The bandwidths ω_x and the frequency δ_1 are kept constant to their measured or specified values. The slope of the dispersive signal A, the integrational feedback parameter α and the current feedback parameter φ are equal for the two curves. Their values are however not accurately known since they include e.g. the frequency response to the piezo voltage and the laser current. By repeating the fit procedure on both curves while iteratively varying A, α and φ, these values were optimized. Values for C are determined to be 0.98(1) and 1.003(5) after optimizing using the spectra and error signals respectively. It is clear that with the first method it is not possible to accurately get C equal to 1, while with the second method this is possible. For both cases the amplitude of the frequency excursion is smaller than Γ. We have successfully tested the technique for frequencies near the extrema of the bandwidth of the AOM. This range thus appears to be the limiting factor. The extent to which C has to be optimized when the frequency jump is changed depends on the linearity of the response of the VCO (AOM frequency) and the laser current on the applied voltage. In practice we had to finetune C slightly when the frequency jump was changed.

Fig. 5.4(b) shows the frequencies of the laser, calculated using Eq. (5.9) for the same parameters as for the two curves in Fig. 5.4(a). The frequency shift of only the AOM is also shown. From Fig. 5.4 it is clear that the error caused by the extra feedback loop is not severe for our application.

The main limiting parameters are the bandwidths ω_{mi} and ω_{ff} in the current feedforward path, which are not present in the electrical path to the AOM. In theory the amplitude of the frequency excursion can be decreased to 0 by better matching the bandwidths of the two paths, so that the detunings due the AOM and the current feedforward path always cancel. It would, of course, be more elegant if the bandwidth ω_V were larger, resulting in a shorter step-up time. However one should be careful with the bandwidths of the current feedforward path and the AOM path, since for constant but unequal bandwidths of these paths the amplitude of the frequency excursions will increase with ω_V.

5.5 Conclusions and outlook

We have demonstrated a new technique for locking a narrow linewidth laser to an arbitrary frequency in the vicinity of a spectral feature not by frequency shifting the output beam, but by frequency shifting the spectroscopy beam. By simultaneously switching the AOM frequency and the laser current it is possible to change the frequency of the laser by more than the locking range, while keeping it locked. Whereas the frequency shifting range in our experiment was limited by the frequency

range of the AOM, it should be possible to make even larger jumps by jumping to a different lock point. The transient frequency excursion was smaller than 5 MHz, less than the linewidth of the ^{87}Rb D_2 transition. The transient time was approximately 0.2 ms. The amplitude of the excursions was limited by the matching of the bandwidths of the electronics in the feedforward path and the AOM path. The duration of the transient was limited by the small bandwidth ω_V of the voltage driving the VCO and the current feedforward. The demonstrated technique is not restricted to diode lasers but should be applicable also to other types of laser, e.g. dye or Ti:Sapphire lasers.

* The technique described in this chapter has not been used in the experiments described in this thesis. However, it is presently being used to lock a Toptica TA100 tapered amplifier system, which is used as the MOT/molasses laser in the setup used for the experiments described in this thesis, and a Tiger laser from Sacher Lasertechnik in another setup in the group.